

Computer aided discrimination between primary and secondary brain tumors on MRI: From 2D to 3D texture analysis

Pantelis Georgiadis¹, Dionisis Cavouras², Ioannis Kalatzis², Dimitris Glotsos², Koralia Sifaki³, Menelaos Malamas³, George Nikiforidis¹, Ekaterini Solomou⁴

¹ Medical Image Processing and Analysis (MIPA) Group, Laboratory of Medical Physics, School of Medicine, University of Patras, Rio, GR-26503 Greece, e-mail: pgeorgiadis@med.upatras.gr

² Medical Image and Signal Processing Laboratory, Department of Medical Instruments Technology, Technological Educational Institute of Athens, Ag. Spyridonos Street, Aigaleo GR-12210, Athens, Greece, e-mail: cavouras@teiath.gr

³ 251 General Hellenic Airforce Hospital, MRI Unit, Katehaki, Athens, Greece

⁴ Department of Radiology, School of Medicine, University of Patras, Rio, GR-26503 Greece

Abstract

Three dimensional texture analysis of volumetric brain MR images have been identified as an important indicator for discriminating among different brain pathologies. The aim of the present study was to evaluate the efficiency of three dimensional textural features using a pattern recognition system in the task of discriminating primary from metastatic brain tissues on T1 post-contrast MRI series. The dataset consisted of sixty seven brain MRI series obtained from patients with verified and untreated intracranial tumors. The pattern recognition system was designed employing a probabilistic neural network classifier, specially modified in order to integrate the non-linear least squares feature transformation logic in its discriminant function. The latter, in conjunction with using three dimensional textural features, enabled boosting up the performance of the system in discriminating primary from metastatic with accuracy of 95.52%. The proposed system might be used as an assisting tool for brain tumor characterization on volumetric MRI series.

Keywords: *brain tumors; MRI; volumetric textural features; pattern classification;*

Introduction

According to a recent statistical report published by the Central Brain Tumor Registry of the United States (CBTRUS), approximately 39,550 people were newly diagnosed with primary benign and primary malignant brain tumors in 2002 [1-3]. Furthermore, in 2000, more than 81,000 people, in the United States alone, were living with a primary malignant brain tumor and 267,000 were living with a primary benign brain tumor. The same report indicates that the incidence rate of primary brain tumors, whether benign or malignant, is 14 per 100,000, while median age at diagnosis is 57 years [3]. Secondary or metastatic brain tumors, in contrast to primary brain tumors, originate in tissues outside

the central nervous system and are a common complication of systemic cancer [1]. Brain metastases outnumber primary brain tumors and are currently classified as the most frequent intracranial tumors. Other studies indicate that brain metastases occur in 20% to 40% of all cancer patients, and that more than 100,000 individuals per year will develop brain metastases [3].

The subjective nature of many of the decisions related with the process of brain tumor characterization has led clinicians to continuously seek for greater accuracy in the pathological characterization of brain tissues mainly from Magnetic Resonance (MR) imaging investigations [4]. The introduction of pattern recognition techniques has enabled experts to extract diagnostic information from the texture of MR images and have been already utilized in previous studies to fulfil the abovementioned need. However, most of the proposed systems are limited in the analysis of textural features derived from 2-dimensional (2D) image slices that include the centre of the tumor despite the fact that the tumor extends in a 3-dimensional (3D) environment. The exploitation of multi-slice volumetric features may offer additional information that will improve the accuracy of these systems.

Regarding MRI brain tumor characterization, 2D textural features have been previously employed in pattern recognition systems for the analysis of brain lesions. More specifically, in a recent study [5], utilizing hierarchical ascending classification with correspondence factorial analysis discrimination accuracies between different tumor types, ranging between 49% (tumors vs oedemas) and 63% (benign vs malignant tumors) were achieved. In another study [4], discriminant analysis and the k-nearest neighbor classifier was used for distinguishing between human brain tumors and oedematous tissues, achieving maximum overall accuracy of 95%. Finally, in a previous study by the authors [6], a two level hierarchical decision tree was employed to discriminate between metastatic brain tumors from gliomas and meningiomas (primary brain tumors) using solely 2D textural features. By using a modified probabilistic neural network classifier discrimination accuracies of 71% (metastatic vs primary tumors) and 81% (gliomas vs meningiomas) were achieved. On the other hand, there has been little work done in the area of characterization and analysis of brain tumor employing features derived from 3D MRI texture. A recent study [7], using a set of six 3D co-occurrence features and linear discriminant analysis, showed improved discrimination accuracies utilizing volumetric features as compared with those obtained by employing the respecting six 2D features between necrosis and solid tumor (100% over 68%) as well as between edema and solid tumor (81% over 57%).

The aim of the present study was to design, implement, and evaluate a pattern recognition system to investigate whether the use of volumetric textural features might improve brain tumor classification accuracy when analyzing routinely taken T1 post-contrast MRI series. By utilizing a Least Squares Features Transformed-Probabilistic Neural Network (LSFT-PNN)-based classification scheme discrimination between secondary (metastatic) and primary brain tumors (meningiomas and gliomas) was performed. These brain tumor categories were selected on the fact that (a) brain metastasis occurs in 20% to 40% of all cancer patients while (b) meningiomas and gliomas are the two higher incidence rated types of benign and malignant primary brain tumors respectively [3].

Materials and methods

Clinical Material

Employing a Siemens Sonata 1.5 Tesla MRI Unit (Siemens, Erlangen, Germany), 67 MR series were obtained from the Hellenic Airforce Hospital with verified untreated intracranial tumors. The dataset comprised 21 cases with metastasis, 19 cases with meningioma, and 27 cases with glioma. From each case, only T1-weighted post-contrast (Gadolinium) series, with Spin Echo (SE) sequence, Echo Time (TE = 15ms), Repetition Time (TR = 500ms) and Slice Thickness (ST = 1.5mm), were used for further analysis. The reason for employing T1 post-contrast series is the increased diagnostic information that they encapsulate in comparison to pre-contrast T1 or T2 weighted series. More specifically, contrast administration assists in the separation of tumor from oedema improving visualization, localization and tumor margin delineation. Contrast enhancement is intense because of the hi-degree of Blood Brain Barrier (BBB) disruption [8].

Feature Extraction

Utilizing these MRI series, an expert radiologist specified cubic Volumes of Interest (VOIs) within each tumor using a software program, developed for the purposes of the present study. The program was designed using the C++ programming language and the Visualization Tool Kit (VTK) [9]. The developed software utilized the marching cubes algorithm [10] to build 3-dimensional models from DICOM MRI series and, thus, to provide the radiologist with a visual aid for segmenting VOIs within brain tumors (Fig. 1). Each segmented VOI was then used to calculate a set of parameters (features) that quantified properties of volume-texture within the brain tumor.

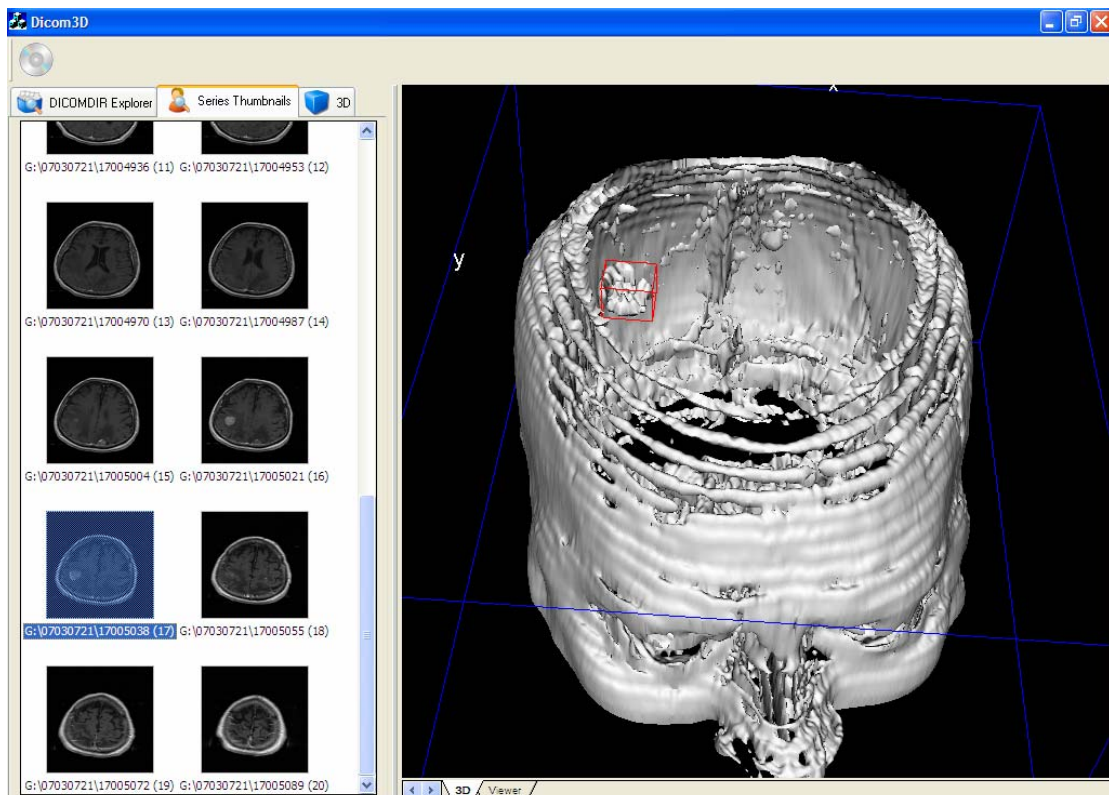


Figure 1: Custom made application for VOI acquisition and volumetric features extraction.

Haralick et. al. [11] and Galloway [12] have described a set of features based on the gray-level co-occurrence and run-length matrices, respectively, to quantify the texture properties of 2D images. The 3D (volumetric) equivalents of these features were calculated in the present study. In a 3D volume, adjacency and consecutiveness can occur in each of 13 directions (compared to 4 directions in a 2D image) and thus 13 gray-level co-occurrence and run-length matrices were generated [7, 13]. Two types of volumetric co-occurrence and run-length features were generated, the average and the range between maximum and minimum over all 13 directions. Additionally, this set was enriched with features derived from the VOI's histogram (mean value, standard deviation, skewness and kurtosis). Therefore, a set of 36 volumetric textural features was used in the present study; 4 features from the VOI's histogram, 22 from the co-occurrence matrices and 10 from the run-length matrices.

Prior classifying volumetric textural features, comparison was performed between the discrimination efficiency of 2D and 3D textural features. To extract the 2D textural features, the central slice of the each VOI was used to calculate the 2D co-occurrence and run-length matrices. Thus, the 36 corresponding with the volumetric, 2D textural features were extracted.

Both 2D and 3D textural features were normalized to zero mean and unit standard deviation [14], according to relation (1)

$$x'_i = \frac{x_i - m}{std} , \quad (1)$$

where x_i and x'_i are the i -th feature values before and after the normalization respectively, and m and std are the mean value and standard deviation, respectively, of feature x_i over all patterns and all classes.

Classification scheme

The PNN classifier [15], encompasses both the Bayes' classification approach and the Parzen's estimators of probability density functions. The discriminant function of the PNN classifier is described by:

$$g_i(\mathbf{x}) = \frac{1}{(2\pi)^{d/2} s^d} \frac{1}{N_i} \sum_{j=1}^{N_i} \exp \left[\frac{\|\mathbf{x} - \mathbf{x}_{ij}\|^2}{2s^2} \right], \quad (2)$$

where \mathbf{x} is the pattern to be classified, \mathbf{x}_{ij} are the training patterns, σ is the spread of the Gaussian activation function (taking values ranging between 0 and 1), N_i is the number of training patterns in class i , and d is the dimensionality of pattern vectors. According to Eq. 2, as the distance between \mathbf{x} and \mathbf{x}_{ij} ($(\mathbf{x} - \mathbf{x}_{ij})^T (\mathbf{x} - \mathbf{x}_{ij})$) increases, the exponential term approaches 0, indicating a small similarity between the two pattern vectors. On the other hand, as the distance between \mathbf{x} and \mathbf{x}_{ij} decreases, the exponential term approaches 1, indicating a significant similarity between the two pattern vectors. As the spread of the Gaussian activation function (σ) approaches 0, even small differences between \mathbf{x} and \mathbf{x}_{ij} will provide a zero value for the exponential term, while larger values of sigma provide more smooth results. The unknown pattern \mathbf{x} is classified to the class with the highest value of the discriminant function $g_i(\mathbf{x})$. PNN's main advantages are that it is fast to train and that data normality is

not a prerequisite. In the training process, neither iterative procedures are used, nor feedback paths are required, since the PNN is a feed-forward and one pass structure [15].

Training patterns \mathbf{x}_{ij} , prior to entering the PNN classifier, were transformed by means of a non-linear least squares feature transformation (LSFT) technique, to render classes more separable by clustering the patterns of each class around arbitrary pre-selected points. The cubic LSFT method is an extension of the linear least squares mapping technique, introduced by [16]. Initially, pattern vectors were extended with third degree elements. Accordingly, if $\mathbf{x} = [x_1 \ x_2 \ \dots \ x_d]$ is a pattern vector, where d is the input space dimensionality, then vector \mathbf{x} was extended with the third degree elements $x_i^3 \ x_i^2 x_j$ and $x_i x_j x_k$, where $i, j = 1, 2, \dots, d$ and $i \neq j \neq k$. The dimensionality of the extended pattern vector ($\hat{\mathbf{x}}$) is equal to [14]:

$$\hat{d} = \frac{(d+3)!}{d!3!} \quad (3)$$

For the formulation of the LSFT 2-class problem, let space \mathbf{S} , with dimensionality equal to the number of classes ($K=2$), and let $\mathbf{P}_i = [p_{i1} \ p_{i2}]$, $i=1,2$ be arbitrary defined points in space \mathbf{S} , corresponding to each class i . A transformation \mathbf{T} is sought such that the total mean square error between the transformed extended vectors ($\mathbf{T}\hat{\mathbf{x}}_{ij}$) and \mathbf{P}_i is minimized as follows:

$$\nabla_{\mathbf{T}} \left[\sum_{i=1}^K \left(\frac{1}{N_i} \sum_{j=1}^{N_i} (\mathbf{T}\hat{\mathbf{x}}_{ij} - \mathbf{P}_i)' (\mathbf{T}\hat{\mathbf{x}}_{ij} - \mathbf{P}_i) \right) \right] = 0 \quad (4)$$

where K is the number of classes, N_i is the number of patterns of class i , and $\hat{\mathbf{x}}_{ij}$ are the 3rd degree extended training patterns of class i . Assuming equal *a-priori* probabilities for each class i , relation (4) results to:

$$\mathbf{T} = \left[\sum_{i=1}^K \left(\frac{1}{N_i} \sum_{j=1}^{N_i} \mathbf{P}_i \hat{\mathbf{x}}_{ij}' \right) \right] \left[\sum_{i=1}^K \left(\frac{1}{N_i} \sum_{j=1}^{N_i} \hat{\mathbf{x}}_{ij} \hat{\mathbf{x}}_{ij}' \right) \right]^{-1} \quad (5)$$

Transformation matrix \mathbf{T} is a $K \times \hat{d}$ matrix, so the decision space dimensionality is equal to the number of brain tumor classes. Following the LSFT procedure, patterns $\hat{\mathbf{x}}_{ij}$ were fed into the PNN classifier, resulting in the final discriminant function of the cubic LSFT-PNN classifier:

$$g_i(\mathbf{x}) = \frac{1}{(2p)^{\hat{d}/2} s^{\hat{d}}} \frac{1}{N_i} \sum_{j=1}^{N_i} \exp \left[\frac{-(\mathbf{T}\hat{\mathbf{x}} - \mathbf{T}\hat{\mathbf{x}}_{ij})' \mathbf{T}(\mathbf{T}\hat{\mathbf{x}} - \mathbf{T}\hat{\mathbf{x}}_{ij})}{2s^2} \right]. \quad (6)$$

Best features combination was determined employing the robust but time consuming exhaustive search method [14], which involves designing the classifier by means of every possible feature-combination, each time evaluating the classifier's performance and finally selecting that feature combination that demonstrated the highest classification accuracy with the smallest number of features. The system's performance was evaluated employing the Leave One Out (LOO) method [14]. Accordingly, the PNN classifier was designed by all but one pattern-vector, which was considered as

unknown and it was classified. The process was repeated, each time leaving-out a different pattern-vector, until all pattern-vectors were thus classified to one of two classes. In this way, the classifier was evaluated by pattern-vectors not involved in its design.

Results

To assess the discrimination efficiency of volumetric features over 2D features a comparative evaluation was performed utilizing the cubic LSFT-PNN classifier. The best overall classification accuracy employing 2D textural features was 89.55%. Individual accuracies in discriminating between primary and secondary brain tumors were 86.96% and 95.24% respectively (Table 1). Best 2D feature vector, used for the optimal design of the LSFT-PNN classifier, comprised correlation, inverse difference moment and sum of squares. Figure 2 shows the scatter diagram of the decision space along with the corresponding decision boundaries for primary and secondary tumors, using 2D textural features and the cubic LSFT-PNN classifier.

Table 1: Cubic LSFT-PNN classifier truth table for discriminating primary and secondary tumors using 2D textural features.

	Primary Brain Tumors	Secondary Brain Tumors	Accuracy (%)
Primary Brain Tumors	40	6	86.96
Secondary Brain Tumors	1	20	95.24
Overall Accuracy			89.55

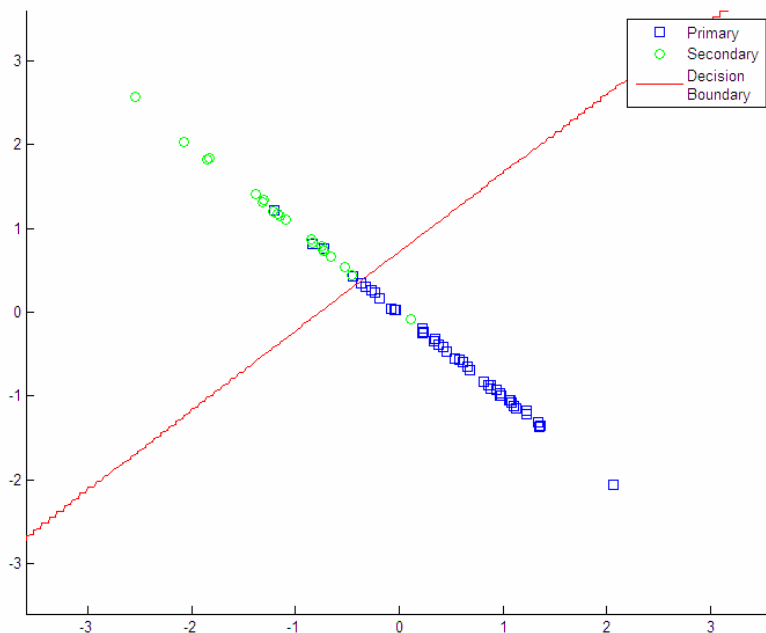


Figure 2: Scatter diagram of the optimum feature combination of the cubic LSFT-PNN classifier and the corresponding decision boundary for discriminating primary from secondary tumors employing 2D textural features.

Three dimensional features increased overall classification accuracy to 95.52% using the same classification scheme. The individual accuracies were 95.65% and 95.24% respectively (Table 2). The best volumetric feature vector comprised skewness, correlation and difference entropy. Figure 3 shows the scatter diagram of the decision space along with the corresponding decision boundaries for primary and secondary tumors, using 3D textural features and the cubic LSFT-PNN classifier.

Comparative classification results are presented in Table 3.

Table 2: Cubic LSFT-PNN classifier truth table for discriminating primary and secondary tumors using 3D textural features.

	Primary Brain Tumors	Secondary Brain Tumors	Accuracy (%)
Primary Brain Tumors	44	2	95.65
Secondary Brain Tumors	1	20	95.24
Overall Accuracy			95.52

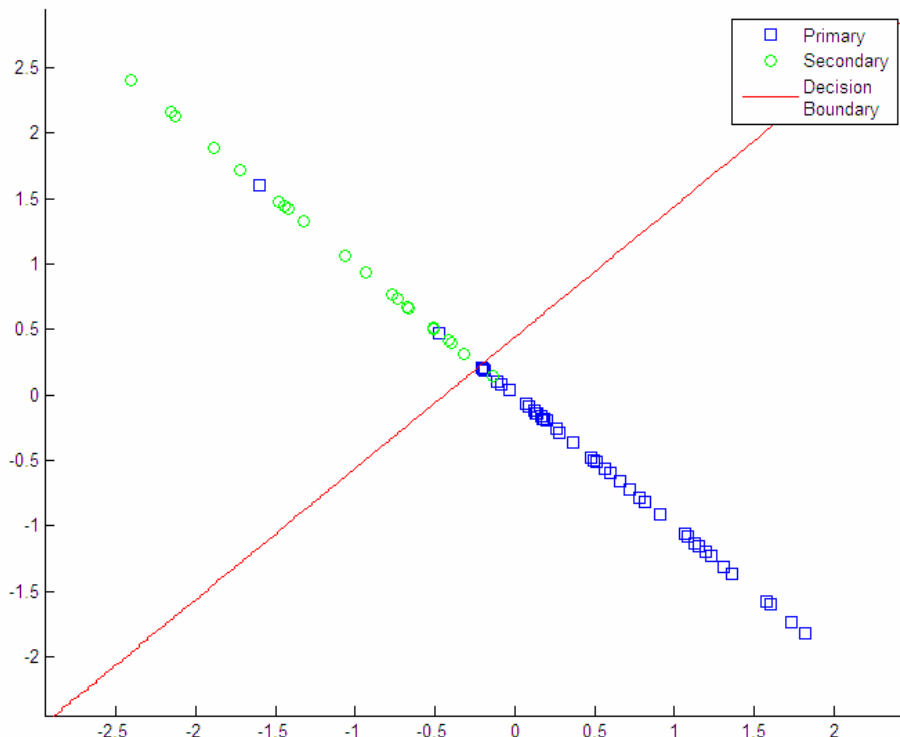


Figure 3: Scatter diagram of the optimum feature combination of the cubic LSFT-PNN classifier and the corresponding decision boundary for discriminating primary from secondary tumors employing 3D textural features.

Table 3: Comparative classification results between 2D and 3D textural features employing the cubic LSFT-PNN classifier.

Number of features	Primary vs Metastatic	
	Overall Accuracy (%)	
	2D Textural Features	3D Textural Features
1	76.12	76.63
2	82.09	85.07
3	89.55	95.52

Discussion

An essential outcome of the present study is that volumetric features have significantly improved classification accuracy in discriminating primary from metastatic tumors as compared to 2D features (improvement from 89.55% to 95.52%). The cubic LSFT-PNN classifier employing volumetric features achieved a sensitivity of 95.65% against 86.96% that achieved employing 2D, assigning 4 more primary brain tumors to the appropriate class. This is important, since the precision of such a decision may be crucial in patient management. Primary and metastatic tumors follow different treatment protocols (radiation therapy and chemotherapy for metastatic tumors while primary tumors may also require surgical intervention [17, 18]).

Features that optimized classification results, encoded information related to the distribution asymmetry around the mean gray-tone value (skewness), the gray-tone linear dependencies (correlation), and the degree of the in-homogeneity of the texture contained in the VOI (difference entropy).

The reason for selecting only the central slice of the VOI in order to extract 2D textural features was to comply with the methodology followed by most previous studies [4, 5]. In this way, we could emphasize the benefits of using 3D textural features, which code information from the whole VOI, compared to selecting just one slice and extracting 2D features from this slice. However, it has to be pointed out that high classification accuracies achieved by 3D texture metrics might be due to the fact that 3D features exploit additional information derived from all available slices (and not just the central slice).

In a recent study [19], an SVM-based classification system discriminated gliomas and meningiomas with 95% overall accuracy, employing as features image intensities from four MR sequences (T1, T2, PD and GD). When features derived from MR spectroscopy were also included, classification accuracy reached 99.8%. In another study [20], employing the LS-SVM classification algorithm and MR spectroscopic data, overall accuracies in distinguishing between secondary brain tumors and meningiomas or glioblastomas or astrocytomas were 97%, 59%, and 96% respectively. Our findings are comparable, however employing solely volumetric textural features from the T1-contrast enhanced MRI series.

Conclusion

The utilization of 3D textural features improved accuracy in the characterization of brain tumors on volumetric MR images as compared to using 2D textural features. The proposed classification system might be used as an assisting tool for brain tumor characterization on volumetric MR images.

Acknowledgements

Funding by the University of Patras Research Committee under the basic research program “K. Karatheodori”, project title “Computer Assisted Diagnosis of Brain Tumors based on Statistical Methods and Pattern Recognition Techniques” is gratefully acknowledged.

References

- [1] Ashby LS, Troester MM, Shapiro WR, (2006), Central nervous system tumors, *Update on Cancer Therapeutics*, 1, 475-513.
- [2] Cruickshank G, (2004), Tumours of the brain, *Surgery (Oxford)*, 22, 69-72.
- [3] Doolittle ND, (2004), State of the science in brain tumor classification, *Semin Oncol Nurs*, 20, 224-230.
- [4] Lerski RA, Straughan K, Schad LR, Boyce D, Bluml S, Zuna I, (1993), MR image texture analysis-an approach to tissue characterization, *Magn Reson Imaging*, 11, 873-887.
- [5] Herlidou-Meme S, Constans JM, Carsin B, Olivie D, Eliat PA, Nadal-Desbarats L, Gondry C, Le Rumeur E, Idy-Peretti I, de Certaines JD, (2003), MRI texture analysis on texture test objects, normal brain and intracranial tumors, *Magn Reson Imaging*, 21, 989-993.
- [6] Georgiadis P, Cavouras D, Kalatzis I, Daskalakis A, Kagadis GC, Sifaki K, Malamas M, Nikiforidis G, Solomou E, (2008), Improving brain tumor characterization on MRI by probabilistic neural networks and non-linear transformation of textural features, *Comput Methods Programs Biomed*, 89, 24-32.
- [7] Mahmoud-Ghoneim D, Toussaint G, Constans JM, de Certaines JD, (2003), Three dimensional texture analysis in MRI: a preliminary evaluation in gliomas, *Magn Reson Imaging*, 21, 983-987.
- [8] Runge V, (2002), *Clinical MRI*, Philadelphia, Saunders.
- [9] Schroeder WJ, Schroeder WJ, Avila LS, Hoffman W, (2000), Visualizing with VTK: a tutorial, *IEEE Computer Graphics and Applications*, 20, 20-27.
- [10] Lorensen W, Cline H, (1987), Marching cubes: A high resolution 3D surface construction algorithm, *Computer Graphics*, 21, 163-169.
- [11] Haralick RM, Shanmugam K, Dinstein I, (1973), Textural Features for Image Classification, *IEEE Trans Syst Man Cybern, SMC-3*, 610-621.
- [12] Galloway MM, (1975), Texture Analysis Using Grey Level Run Lengths, *Comp. Graph. and Image Proc*, 4, 172-179.

- [13] Xu DH, Kurani A, D. FJ, S. RD, (2004), Run-length encoding for volumetric texture, In: Proceedings of the 4th IASTED International Conference on Visualization, Imaging, and Image Processing - VIIP 2004.
- [14] Theodoridis S, Koutroumbas K, (1999), *Pattern Recognition*, New York, Academic Press.
- [15] Specht DF, (1990), Probabilistic Neural Networks, *Neural Networks*, 3, 109-118.
- [16] Ahmed N, Rao R, (1975), *Orthogonal Transforms for Digital Signal Processing*, NY, Springer-Verlag.
- [17] Peacock K, Lesser G, (2006), Current therapeutic approaches in patients with brain metastases, *Current Treatment Options in Oncology*, 7, 479-489.
- [18] Graham CA, Cloughesy TF, (2004), Brain tumor treatment: Chemotherapy and other new developments, *Semin Oncol Nurs*, 20, 260-272.
- [19] Devos A, Simonetti AW, van der Graaf M, Lukas L, Suykens JA, Vanhamme L, Buydens LM, Heerschap A, Van Huffel S, (2005), The use of multivariate MR imaging intensities versus metabolic data from MR spectroscopic imaging for brain tumour classification, *J Magn Reson*, 173, 218-228.
- [20] Devos A, Lukas L, Suykens JA, Vanhamme L, Tate AR, Howe FA, Majos C, Moreno-Torres A, van der Graaf M, Arus C, Van Huffel S, (2004), Classification of brain tumours using short echo time 1H MR spectra, *J Magn Reson*, 170, 164-175.